Decoherence and correspondence in conservative chaotic dynamics

Jiangbin Gong and Paul Brumer
Chemical Physics Theory Group, University of Toronto, Toronto, Canada M5S 3H6
(Received 3 November 1998; revised manuscript received 19 March 1999)

The quantum and classical dynamics of a conservative nonlinear Hamiltonian system in the chaotic regime are compared in the absence and presence of decoherence effects. Results show marked improvement in classical-quantum correspondence with the introduction of decoherence, even though the initial quantum dynamics is far from the semiclassical limit. [S1063-651X(99)09208-9]

PACS number(s): 05.45.−a, 03.65.Bz, 03.65.Sq, 05.40.−a

I. INTRODUCTION

The means by which quantum mechanics approximates classical mechanics for macroscopic systems remains a subject of considerable interest. Traditional, often heuristic, approaches argue that the equations of classical mechanics emerge naturally as the de Broglie wavelength becomes small. Strong mathematical support for this approach, but with the necessary inclusion of infinitesimal averaging over energy, has recently been given [1]. By contrast, others argue that classical mechanics is not a limiting case of quantum mechanics, but rather that decoherence, i.e., loss of coherence due to coupling to other degrees of freedom, is necessary to ensure the validity of the correspondence principle [2–4]. This proposal, however, is the topic of considerable controversy, with many arguing that the relationship between decoherence and correspondence is tenuous [5].

In this paper we examine a nonlinear oscillator system in the chaotic regime and show that decoherence does indeed lead to substantially improved agreement between classical and quantum mechanics. This constitutes a major extension of previous work on the effect of decoherence, which was limited to one-dimensional driven chaotic systems [6–11]. In particular, our extension is to the broad class of conservative nonlinear Hamiltonian systems, and into the domain where the system is far from the semiclassical regime. In addition, we develop a quantum state diffusion-split operator method that provides a generally useful and efficient method for studying decoherence and gives interesting insights into the origins of decoherence in conservative systems.

To consider the effects of decoherence we adopt the model of Caldeira and Leggett and of Uhruh and Zurek [12] in which the system interacts with a harmonic bath in the weak coupling and high temperature limit. Extending this model to a system with two degrees of freedom gives the time evolution of the density matrix $\hat{\rho}$ in the Wigner representation as [12]

$$\frac{\partial \rho^W}{\partial t} = \{H, \rho^W\} + \sum_{(l_1+l_2)\ \text{odd}} \frac{(\hbar/2i)^{(l_1+l_2-1)}}{l_1! l_2!} \frac{\partial^{(l_1+l_2)} V(x,y)}{\partial x^{l_1} \partial y^{l_2}} \times \frac{\partial^{(l_1+l_2)} \rho_W}{\partial p_x^{l_1} \partial p_y^{l_2}} + D\left(\frac{\partial^2 \rho^W}{\partial p_x^2} + \frac{\partial^2 \rho^W}{\partial p_y^2} \right). \quad (1)$$

Here (p_x, p_y, x, y) are the system momenta and coordinates, $V(x,y)$ is the potential contribution to the Hamiltonian H, and $\rho^W = \rho^W(p_x, p_y, x, y; t)$ is the Wigner representation of the density matrix $\hat{\rho}$. The first term on the right hand side of Eq. (1) is the classical Poisson bracket which generates classical dynamics, the second term is responsible for quantum/classical differences, and the third term induces decoherence. By using Eq. (1), and by imposing restrictions on the derivatives of the potential to ensure the second term is small relative to the Poisson bracket term, Zurek and Paz [2] (and independently, Kolovsky [13]) derived the following condition for the quantum transition to classical behavior in chaotic systems:

$$\sqrt{\frac{2D}{\lambda}} \chi > \hbar, \quad (2)$$

where λ is the Lyapunov exponent of the classical dynamics, and χ is a characteristic potential length, defined, for the one degree of freedom system that they examined, as the average value of $\sqrt{|\partial_x V / \partial_x^3 V|}$. Below we use this criterion to establish the range of relevant parameters in our numerical studies.

Note that Eq. (1) ignores the back action of the system on the environment. As such, one can show [14] that the system absorbs energy from the environment at a D-dependent rate. Thus, since D is required to be sufficiently large to satisfy Eq. (2), then observable energy absorption is a necessary characteristic of decoherence (without dissipation) in the quantum regime of non-negligible $\hbar$. In the case chosen below the rate is D/m [14] per degree of freedom, where m is the mass, a theoretical prediction which we use to confirm the energy absorption observed computationally.

II. QUANTUM STATE DIFFUSION-SPLIT OPERATOR APPROACH

Solving Eq. (1) is quite complicated for a typical two degree of freedom chaotic system. A useful numerical technique for carrying this out, as well as the specific example of interest, is described in this section.

The particular case we examine is given by the nonlinear oscillator Hamiltonian [16]

$$H = \frac{1}{2}(p_x^2 + p_y^2 + \alpha x^2 y^2) + \frac{\beta}{4}(x^4 + y^4), \quad (3)$$

with $\beta = 0.01$, $\alpha = 1.0$, a regime where the system is fully chaotic [16] with $\lambda \approx 0.5$. Results were also obtained for $\alpha = 0.1$ where the system is still chaotic but where the

Lyapunov exponent is approximately two times smaller. This system is particularly useful for decoherence studies because (a) it has the simple energy scaling property that all trajectories can be scaled onto one Poincaré surface of section, ensuring that the dynamics is essentially the same even if the system energy changes due to system-environment interaction; (b) the dynamics of this system at $\alpha=1.0$ is very chaotic, enhancing the classical-quantum discrepancy for the closed system and allowing for a study in the quantum regime; (c) the potential has no simple harmonic terms. Thus, any observed agreement between classical and quantum behavior cannot be attributed to the similarity of classical and quantum harmonic oscillator dynamics.

To solve Eq. (1) we adapt the quantum state diffusion (QSD) approach [15] based on the stochastic differential equation for the state vector into a usable scheme for nonlinear oscillator systems. In this approach we solve for the dynamics of the system wave function in the presence of a random potential, to obtain a single realization $|\psi(\xi_m(t),t)\rangle$. Specifically, we consider [15]

$$|d\psi\rangle=\frac{-i}{\hbar}H|\psi\rangle dt + \sum_m (2\langle L_m^\dagger\rangle_{|\psi\rangle}L_m - L_m^\dagger L_m - \langle L_m^\dagger\rangle_{|\psi\rangle}\langle L_m\rangle_{|\psi\rangle})|\psi\rangle dt + \sum_m (L_m-\langle L_m\rangle_{|\psi\rangle})|\psi\rangle d\xi_m, \quad (4)$$

where the operators L_m represent the coupling between the system and environment, and $\langle L_m\rangle_{|\psi\rangle}=\langle\psi|L_m|\psi\rangle/\langle\psi|\psi\rangle$ and where $d\xi_m$ are independent complex differential random variables of a complex normalized Wiener process, with well defined mean properties [15]. Averaging over these realizations by selecting different $d\xi_m$ gives $\rho(t)=(1/S)\Sigma_{\xi_m}|\psi(\xi_m(t),t)\rangle\langle\psi(\xi_m(t),t)|$, with S being the total number of realizations of the time-dependent stochastic variables ξ_m. Note that the $\rho(t)$ is the sum of projection operators computed from individual realizations so that one can regard each contribution $|\psi(\xi_m(t),t)\rangle\langle\psi(\xi_m(t),t)|$ as representing a single laboratory experiment for a quantum open system. Below we utilize this viewpoint to gain insight into the effects of decoherence on the evolution of individual wave packets.

Our specific implementation of the QSD method takes the operators L_i as $L_1=(\sqrt{D}/\hbar)\hat{x}$ and $L_2=(\sqrt{D}/\hbar)\hat{y}$ and uses the first-order Euler method, shown to be accurate for statistical expectation values [17], to integrate Eq. (4). That is, we solve

$$|\psi(t+\delta t)\rangle=\exp(-iH\delta t/\hbar)|\psi(t)\rangle + \frac{D}{\hbar^2}(2\langle x\rangle x-x^2-\langle x\rangle^2)|\psi(t)\rangle + \frac{\sqrt{D}}{\hbar}(x-\langle x\rangle)|\psi(t)\rangle W_1+\frac{D}{\hbar^2}(2\langle y\rangle y-y^2 -\langle y\rangle^2)|\psi(t)\rangle + \frac{\sqrt{D}}{\hbar}(y-\langle y\rangle)|\psi(t)\rangle W_2, \quad (5)$$

where δt is the integration time step, and where W_1, W_2 are two ordinary independent complex random variables with (where M denotes the mean) $M((\mathrm{Re}\,W_1)^2)=M((\mathrm{Im}\,W_1)^2)=M((\mathrm{Re}\,W_2)^2)=M((\mathrm{Im}\,W_2)^2)=\delta t$; $M(W_1)=M(W_2)=0$. The Hamiltonian dynamics is carried out via the split operator fast Fourer transform (FFT) technique [18]. Thus, combining the FFT approach and the Euler integration scheme gives a general systematic approach to the wave packet dynamics in the quantum state diffusion picture for nonlinear oscillator systems, even far from the semiclassical limit.

Below we compare these results to classical mechanics by obtaining the classical phase space density $\rho_t(x,y,p_x,p_y)$ which satisfies the Fokker-Planck equation:

$$\frac{\partial}{\partial t}\rho_t(x,y,p_x,p_y) =\{H,\rho_t(x,y,p_x,p_y)\} + D\left(\frac{\partial^2}{\partial p_x^2}\rho_t(x,y,p_x,p_y)+\frac{\partial^2}{\partial p_y^2}\rho_t(x,y,p_x,p_y)\right). \quad (6)$$

In the closed system case ($D=0$) we do this by solving Hamilton's equations to obtain the classical trajectories; 5×10^4 trajectories were found sufficient for convergence. Similarly, in the open system case ($D\neq0$) ρ is obtained by integrating the Langevin-Itô equations for each sample trajectory:

$$dx=\frac{\partial H}{\partial p_x}dt,\quad dy=\frac{\partial H}{\partial p_y}dt,$$
$$dp_x=-\frac{\partial H}{\partial x}dt+\sqrt{2D}\,\eta_1,\quad dp_y=-\frac{\partial H}{\partial y}dt+\sqrt{2D}\,\eta_2. \quad (7)$$

Here $\eta_i, i=1,2$ are independent real differential stochastic variables satisfying $M(\eta_1)=M(\eta_2)=0$, $M(\eta_1^2)=M(\eta_2^2)=dt$. Once again, Monte Carlo sampling from the initial distribution and Euler integration of Eq. (7) gave converged results for ρ with $(2-4)\times10^4$ sample trajectories and a total of 30 to 50 realizations of η_1 and η_2 for each sample trajectory.

III. COMPUTATIONAL RESULTS

As a specific example we chose to examine quantum-classical correspondence using an initial $\psi(x,y,0)$ given as a two-dimensional coherent state with Wigner function,

$$\rho_0(x,y,p_x,p_y)=\left(\frac{1}{\pi^2}\right)\exp\left(-\frac{(x-\overline{x})^2}{\hbar}-\frac{(y-\overline{y^2})}{\hbar} -\frac{(p_x-\overline{p}_x)^2}{\hbar}-\frac{(p_y-\overline{p}_y)^2}{\hbar}\right), \quad (8)$$

where $\overline{x}$, $\overline{y}$, $\overline{p_x}$, and $\overline{p_y}$ are mean positions and momenta, respectively. In the computations reported below [19] $\hbar=0.1$, $\Delta t=0.002$, $D=6\times10^{-4}$, $\overline{x}=0.40$, $\overline{y}=0.60$, $\overline{p_x}=0.50$, $\overline{p_y}=0.414$ with a spatial grid spacing of $\Delta x=\Delta y$

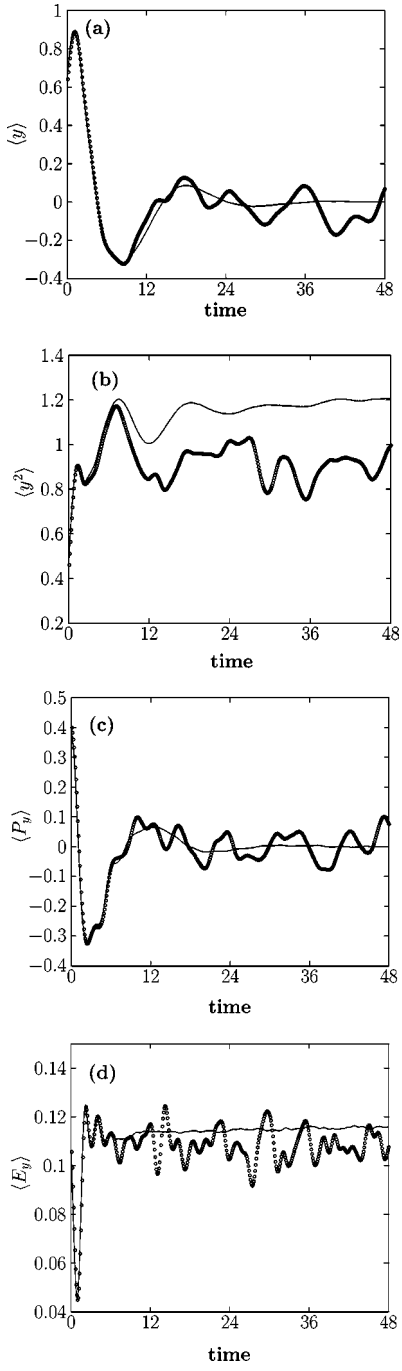

FIG. 1. Time dependence of four statistical moments ($\langle y \rangle$, $\langle y^2 \rangle$, $\langle P_y \rangle$, and $\langle E_y \rangle$) for the closed chaotic system case. Dark dots denote quantum results, thin solid lines are classical results. All variables are in dimensionless units [19].

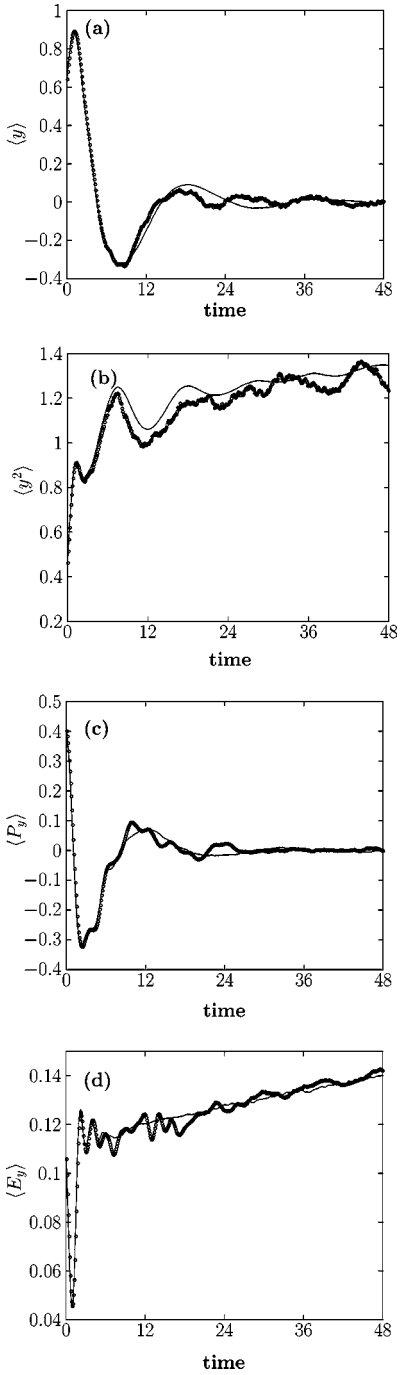

FIG. 2. Same as Fig. 1, but for the open chaotic system case.

$=0.16$. Convergence was checked by decreasing the time steps, enlarging the grid size, and by increasing S, with $S=1000$ found sufficient to obtain convergent results. In addition, energy absorption was in accord with the theoretical prediction cited above.

Note first that our choice of D lies close to the border of the quantum-classical transition predicted by Eq. (2). That is, this two-dimensional system has three characteristic potential lengths χ, $\sqrt{|\partial_x V/\partial_x^3 V|}$, $\sqrt{|\partial_x V/\partial_x^2 \partial_y V|}$, and $\sqrt{|\partial_x V/\partial_x \partial_y^2 V|}$. For the energy region of interest their average values are 8, 1.5, and 1, respectively. With $\lambda \approx 0.5$ for $\alpha=1.0$ and approximately two times smaller for $\alpha=0.1$, the inequality (2) is satisfied for at least one of these lengths.

We consider first a comparison of classical and quantum mechanics for the closed (i.e., $D=0$) system, as shown through expectation values of coordinates and momenta and ''energy in a zeroth-order mode,'' e.g., for y, $\langle E_y \rangle = \langle p_y^2/2 + (\beta/4) y^4 \rangle$. Figure 1 shows the classical and quantum expectation values for four moments associated with y. Analogous results were obtained in the x variable. All figures show qualitatively similar behavior, i.e., after an initial period of classical/quantum agreement the quantum results continue to oscillate while the classical results show smooth relaxation [20]. Computational results in the less chaotic regime ($\alpha=0.1$) showed similar results except that the deviation be-

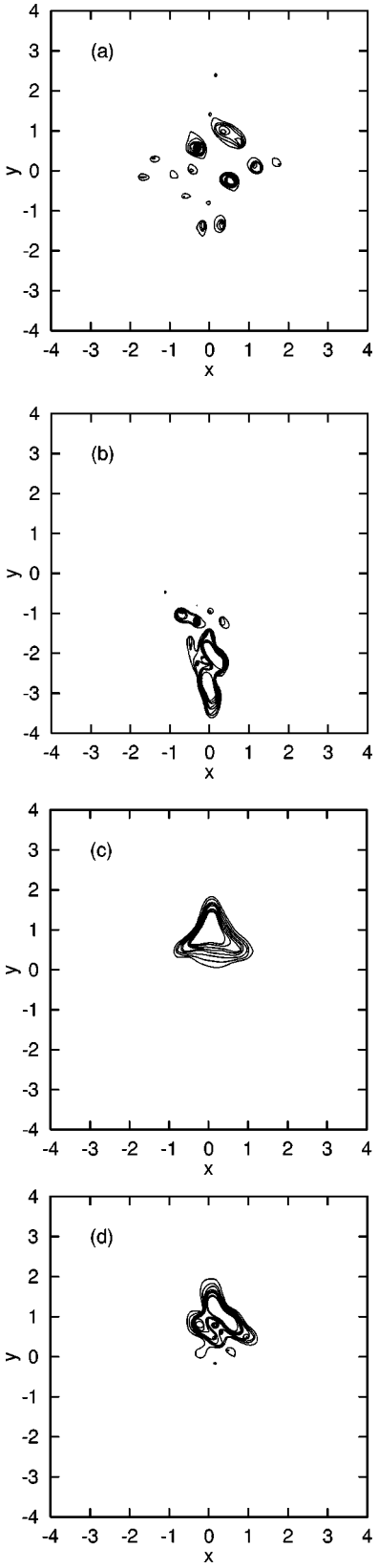

FIG. 3. Contours of constant wave function intensity at $t=25$ for propagation, for the chaotic case, from the same initial state: (a) shows results for the closed system ($D=0$); (b), (c), and (d) show results for different realizations with nonzero D. All variables are in dimensionless units [19].

tween the classical and quantum is significantly less in the $\alpha=0.1$ case, and the classical-quantum discrepancy begins at a later time. Note also that the quantum results do not always simply oscillate about the classical (e.g., see results for $\langle y^2\rangle$) and that the quantum fluctuations about the mean are substantial (e.g., 30% in the case of $\langle E_y\rangle$).

Results for the same moments, after introducing decoherence, are shown in Fig. 2. A comparison of Figs. 1 and 2 shows substantially improved classical-quantum correspondence upon introducing decoherence. In particular, Fig. 2(a) and Fig. 2(c) show that quantum oscillations in the first-order moments are strongly suppressed by decoherence. More remarkable is the observed correspondence for the case of $\langle y^2\rangle$ [see Fig. 2(b)], in which the long term quantum average in the closed system deviated significantly from the long term classical average. This indicates decoherence delocalizes quantum distribution functions within the energy shell, a conservative-system analog of the noise-induced delocalization seen in one-dimensional quantum chaotic systems [6,7,9]. Finally, the correspondence in $\langle E_y\rangle$ is shown in Fig. 2(d), suggesting that the energy transfer between different degrees is also strongly affected by decoherence effects. We also note that similar improved agreement was obtained for moments of x and for the $\alpha=0.1$ case.

Further insight into the effect of decoherence results from examining individual realizations within the QSD approach. For example, Fig. 3 shows four quantum wave functions at $t=25$, each emerging from the same time zero initial wave function. Figure 3(a) shows the result of propagation in the absence of decoherence and Figs. 3(b)–3(d) show three different $|\psi(\xi_m(t),t)\rangle$ at $t=25$, a time by which decoherence appears to have restored considerable correspondence (see Fig. 2). A comparison of Figs. 3(b)–3(d) with Fig. 3(a) shows that the former has far less structure than the latter; indeed Fig. 3(c) shows that decoherence has changed the complex structure in Fig. 3(a) into a single peak. In essence, the competition between the Hamiltonian chaos (which tends to exponentially [21] increase the wave packet structure) and the stronger decoherence effect (which tends to suppress the wave packet structure) is vividly demonstrated here.

Note, finally, that since the parameters chosen above lie in the range expected of a typical molecule, our results suggest the possibility of experimentally observing these effects in the vibrational motion of excited polyatomics. To see this, note that a convenient dimensionless unit to compare systems is the fraction $F(t)$ of energy absorbed per degree of freedom from the bath per vibrational oscillatory period $2\pi/\omega$, relative to the level spacing $\hbar\omega$, where ω is the vibrational period. That is, $F(t)=(D/m)(2\pi/\omega)(1/\hbar\omega)$. From Eq. (2) we have

$$F(t)=2\pi D/(m\hbar\omega^2)>\pi\hbar\lambda/(m\chi^2\omega^2)\approx\pi\hbar/(\chi^2 m\omega), \tag{9}$$

where we have assumed [22] $\lambda\approx\omega$. Typical sizes of the right hand side of the equation for a small molecule are on the order of 10^{-3}, in the same range as that obtained for the model adopted in this paper. With the right hand side of Eq. (9) being the ratio of $\hbar$ to a typical system action, the small molecule is seen to be of the same order of ''quantumness'' as the adopted model.

IV. SUMMARY

We have shown for a generic conservative chaotic Hamiltonian system that decoherence does indeed lead to significant improvement in classical-quantum correspondence. That is, the tendency for the evolving phase space distribution in chaotic dynamics to fragment exponentially fast is compensated by the smoothing effect of the externally induced decoherence and classical-quantum agreement is significantly improved. Indeed, the stronger the chaos, and hence the fragmentation, the more effective is the decoherence [23], so the balance between them is expected to be retained over a wide range of λ. This is the case even though our studies are in the quantum regime so that the required magnitude of the decoherence leads to substantial difference between the classical results in the presence and absence of decoherence. Nonetheless, correspondence is much improved by the decoherence effects, i.e., *quantum mechanics plus decoherence effects* is in far better agreement with the *classical mechanics plus decoherence effects* than is the analogous comparison in the absence of decoherence. This agreement is expected to improve even further as one approaches the classical limit.

ACKNOWLEDGMENTS

We thank the Natural Sciences and Engineering Research Council of Canada and the U.S. Office of Naval Research for support of this research.

[1] J. Wilkie and P. Brumer, Phys. Rev. A **55**, 27 (1997); **55**, 43 (1997).
[2] W.H. Zurek and J.P. Paz, Phys. Rev. Lett. **72**, 2508 (1994); **75**, 351 (1995).
[3] W.H. Zurek, http://xxx.lanl.gov, e-print quant-ph/9802054.
[4] D. Giulini, E. Joos, C. Kiefer, J. Kupsch, I.O. Stamatescu, and H.D. Zeh, *Decoherence and the Appearance of a Classical World in Quantum Theory* (Springer, Berlin, 1996).
[5] See Letters to the Editor in Phys. Today **46** (4), 81 (1993).
[6] E. Ott, T.M. Antonsen, Jr., and J.D. Hanson, Phys. Rev. Lett. **53**, 2187 (1984).
[7] D. Cohen, Phys. Rev. A **43**, 639 (1991); **44**, 2292 (1991).
[8] K. Shiokawa and B.L. Hu, Phys. Rev. E **52**, 2497 (1995).
[9] R. Graham and S. Miyazaki, Phys. Rev. A **53**, 2683 (1996); P. Goetsch and R. Graham, *ibid.* **54**, 5345 (1996).
[10] L. Bonci, P. Grigolini, A. Laux, and R. Roncaglia, Phys. Rev. A **54**, 112 (1996).
[11] S. Habib, K. Shizume, and W. Zurek, Phys. Rev. Lett. **80**, 4361 (1998).
[12] A.O. Caldeira and A.J. Leggett, Physica A **121**, 587 (1983); W.G. Unruh and W.H. Zurek, Phys. Rev. D **40**, 1071 (1989); B.L. Hu, J.P. Paz, and Y. Zhang, *ibid.* **45**, 2843 (1992); **47**, 1576 (1993).
[13] A.R. Kolovsky, Europhys. Lett. **27**, 79 (1994); Phys. Rev. Lett. **76**, 340 (1996).
[14] J.C. Flores, Europhys. Lett. **29**, 653 (1995).
[15] N. Gisin and I. Percival, J. Phys. A **25**, 5677 (1992), and references therein.
[16] See, e.g., B. Eckhardt, G. Hose, and E. Pollak, Phys. Rev. A **39**, 3776 (1989).
[17] G.N. Milstein, *Numerical Integration of Stochastic Differential Equations* (Kluwer, Dordrecht, 1995).
[18] M.D. Feit, J.A. Fleck, and A. Steiger, J. Comput. Phys. **47**, 412 (1982).
[19] Note that we begin with a dimensionless scaled Hamiltonian [Eq. (3)]. As a result, all relevant variables are understood to be dimensionless and scaled. The relation between the scaled variables and unscaled variables is, however, crucial for retrieving specific units when necessary. For a general Hamiltonian $\tilde{H}=\tilde{p}_x^2/2m_1+\tilde{p}_y^2/2m_2+\tilde{V}(\tilde{x},\tilde{y})$ with all variables with tildes denoting ordinary unscaled variables, we can define the dimensionless scaled variables $x\equiv\sqrt{m_1\omega/\ell}\tilde{x}$, $p_x\equiv\sqrt{1/m_1\omega\ell}\tilde{p}_x$, $y\equiv\sqrt{m_2\omega/\ell}\tilde{y}$, and $p_y\equiv\sqrt{1/m_2\omega\ell}\tilde{p}_y$. Here ℓ has units of action, and m_i and ω are ordinary constants with units of mass and frequency. Typically, ω is taken as the average frequency of this system and ℓ is taken to scale the true Planck constant; that is, $\hbar=\tilde{\hbar}/\ell$, where $\tilde{\hbar}$ is the ordinary Planck constant and $\hbar$ is the dimensionless scaled Planck constant. The scaled variables satisfy the canonical equations of motion for the scaled time $t=\omega\tilde{t}$ and the scaled Hamiltonian $H=\tilde{H}/\ell\omega$. For quantum descriptions one can verify that $[x,p_x]=i\hbar$, $[y,p_y]=i\hbar$.
[20] Analogous results were observed previously for the stadium billiard. See K.M. Christoffel and P. Brumer, Phys. Rev. A **33**, 1309 (1985).
[21] J. Gong and P. Brumer (unpublished).
[22] P. Brumer and M. Shapiro, Adv. Chem. Phys. **70**, 365 (1988).
[23] A.K. Pattanayak and P. Brumer, Phys. Rev. Lett. **79**, 4131 (1997).